ORIGINAL PAPER

Integrated design and prototyping of a robotic eye system for ocular and craniofacial trauma simulators

Marcello Gallerani[1] · Greta Vazzoler[2,3] · Gianluca De Novi[1] · Roberto Razzoli[2] · Giovanni Berselli[1,2] · Mark P. Ottensmeyer[1]

Abstract

This article presents the development of a prototype robotic eye-motion system for a novel simulator of ocular and craniofacial trauma that was developed for practical skills training of eye surgeons and first responders. The simulator fills a gap in the ophthalmological training domain, specifically between virtual reality-based systems for cataract and retinal repair and part-task trainers without quantitative measurement capabilities. Combining physical anatomical modules, instrument tracking and embedded sensors with a data acquisition/feedback system in a portable bench-top structure, it offers an alternative to animal- and cadaver-based training. The prototype robotic eye system described includes multiple human eye globe motion features: eye pitch and yaw motion, proptosis, and sensing of applied force to detect pressure/load applied to the globe.

Keywords Simulation-based-training · Virtual and physical prototyping · Medical robotics · Computer-aided design

1 Introduction

A major contributor to the morbidity and mortality of US armed forces injured during hostile action has been traumatic injuries to the head, face, and neck even though these areas comprise only 12% of the total body surface area [1, 2]. While body armour improvements have reduced injuries to the trunk and extremities, the face and head remain relatively less protected. A lack of realistic simulators for treating facial and head damage leaves medics and physicians with few opportunities to train before operating on patients. Most of the simulators are applied in monitored environments, e.g., hospital operating rooms. In a warzone, the first minutes after the occurrence of severe injuries are crucial for saving the patient, hence the need to have already developed the necessary skills. Military ophthalmologists and other physicians who may be called on to treat eye injuries have a need to develop trauma skills since critical competence in certain skills including microsurgical suturing are now taught less frequently in US residencies, hence, the need to develop a new prototype training system that can cover these situations. In this context, a novel system for training was developed to simulate injuries to the orbit and peri-orbital tissue injuries as well as facial trauma including elements of the mandible, maxilla, and upper airway. This paper presents the development of the robotic system supporting the ocular elements of the simulator.

✉ Giovanni Berselli
  giovanni.berselli@unige.it

  Marcello Gallerani
  marcello.gallerani@gmail.com

  Greta Vazzoler
  greta.vazzoler@edu.unige.it

  Gianluca De Novi
  denovi.gianluca@mgh.harvard.edu

  Roberto Razzoli
  roberto.razzoli@unige.it

  Mark P. Ottensmeyer
  mottensmeyer@mgh.harvard.edu

1 Department of Imaging, Massachusetts General Hospital and Harvard Medical School, 65 Landsdowne Street, Cambridge, MA 02139, USA

2 Department of Mechanical, Energy, Management and Transportation Eng, University of Genova, Via All'Opera Pia 15a, 16145 Genoa, Italy

3 Institute of Mechanical Intelligence, Scuola Superiore Sant'Anna, Via Alamanni 13b, 56010 Pisa, Italy

Fig. 1 OCF initial set-up: unanimated mannequin and instrumentation

Fig. 2 OCF head. Skull comparison: **a** CT; **b** CAD model; **c** physical prototype

1.1 System overview

This research developed a prototype of a novel Ocular and CranioFacial trauma (OCF) simulator for use by eye surgeons and first responders in treating injuries to the face and eyes, aiming at training, and maintaining practical skills. The prototype combines physical anatomical modules with instrument tracking sensors along with a data acquisition, scoring and feedback system in a portable bench-top structure [3]. The main purpose of this study was to design a functional prototype OCF simulator offering procedural training in a quantifiable and reproducible form in a safe environment. The OCF was designed for integration with training methods that may improve additional medical surgery skills, such as soft tissue injury treatment and upper airway management, without risk to actual patients or need for animal-based training. The training is based on an advanced assessment method, which scores users' expertise to validate their procedures and improve their skills. This approach uses surgical instruments, surgeon movement tracking technology, sensors, and an augmented reality system to provide feedback and guidance to the surgeon [4]. The simulator initial set-up is shown in Fig. 1: it is a hybrid physical/virtual system for surgical technique learning that includes an unanimated mannequin head with replaceable eye trauma modules, force sensors and position/orientation-tracked instruments with a closure function. Figure 2 depicts: the OCF's underlying skull form, which was derived from a deidentified Computed Tomography (CT) scan of a real person; the anatomy manipulated in a CAD environment illustrating elements supporting simulated fractures; and the skull and upper mandible of the simulator prototype into which the robotic eye system was installed. The original simulator included a passive silicone left eye module (Fig. 1, left), while the new robotic system includes both left and right eyes and is covered by a fully replaceable silicone face with simulated lacerations (Fig. 1,
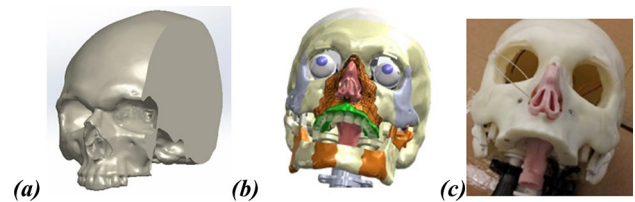
right). The passive and full-face components are made from several layers of silicon to simulate the human skin tissue. In some configurations, tear and lacrimal ducts and vessels are included in the skin to recreate visual, tactile and functional aspects of a real face for simulated surgery operations. For versions supporting procedures such as lateral canthotomy and cricothyroidotomy, sensors are fused into the silicon to allow detecting incision length and direction, providing useful feedback for the trainee.

The present research focuses on the conceptual design and physical prototyping of a novel eye simulator, the "EYE-MECH" shown in Fig. 3a. It uses an electromechanical system designed to simulate the behaviour and movements of human eyes. Dynamic pupils have been realized for the simulator eyes that respond to a light-level sensor, enhancing the realism of the simulated patient. As shown in Fig. 3b, the eye mechanism is mounted into a cavity in the skull form. The skull CAD model was extracted from a CT scan, which was segmented using *Mimics* (Materialise, Leuven, Belgium), exported to STL format, and imported into *Solidworks* (Dassault Systemes Solidworks Corp., Waltham, USA) for CAD modelling, thus ensuring that the EYE-MECH was designed based on realistic anatomical dimensions.

Aiming at accurately reproducing the behaviour of human eyes, the design of an ocular robotic system is a challenging project involving several engineering choices. An eye motion mechanism can be realized in different ways, according to the final purpose and its basic requirements. To cope with limitations of the current state of the art and realize a novel eye simulator, this paper focuses on the following main points:

- *Human anatomy*: Sect. 2 presents the anatomy of the eye with its main features, functionality, and range of motion (RoM). This knowledge is of great importance when designing the device and motivated the design choices of the eye system simulator.
- *State of the art:* A brief review of the available systems from the literature was carried out to analyse pros and cons of various approaches and is reported in Sect. 3.
- *Proof of concept and mechanism design*: the mechanism design and prototyping are deeply studied in Sect. 4. The main features to be replicated and requirements for designing a reliable and realistic system were defined according
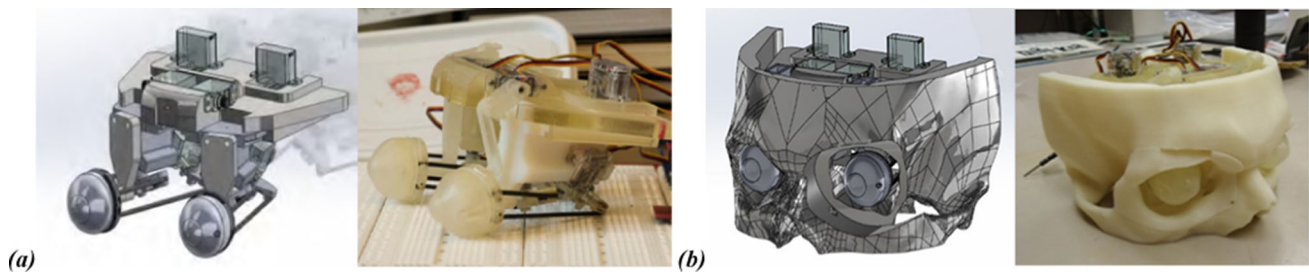
Fig. 3 CAD model and physical prototype of **a** the EYE-MECH; **b** the assembled skull (EYE-MECH into the skull cavity)

to the previous points so that the mechanism would be designed, sized, and properly integrated within the constraints of human anatomy.

- *Physical prototyping, control system, and tests*: Sect. 4 describes the mechanism components that were prototyped using 3D printing and conventional machining and assembled to obtain a working prototype. An Arduino Duemilanove (Arduino, Turin, Italy) was used to control and test the device's functionality and reliability.

2 Human eye anatomy

2.1 Eye mechanism

To study the human eye's anatomy, this section focuses on two main aspects:

- *Eye muscular system*: Number, position and functions of the muscles engaged in the eye motion were inspected to collect data about the muscular system RoM and speed and average eyeball dimensions.
- *Traumatic proptosis*: Causes and symptoms of the condition were studied, along with the medical procedure to treat them.

Eye muscular system [5]: The human eyeball is controlled by a group of six of the seven muscles of the orbit, shown in Fig. 4 [6]. Four of these muscles (from 1 to 4) primarily control the elevation, depression, adduction, and abduction movement of the eye, respectively the up, down, inwards/medial, and outwards/lateral directions. They cooperate in providing the eye with two rotational Degrees of Freedom (DoFs). Two muscles (5 and 6) principally provide limited rotation (torsion) about the axis of the eye. One extremity of each of these muscles is attached to the sclera of the eyeball, whereas the other ends are attached to the tendonous annulus of Zinn which encircles the optic and oculomotor nerves and ophthalmic artery. The seventh muscle of the orbit is the Levator Palpebrae Superioris, and its function
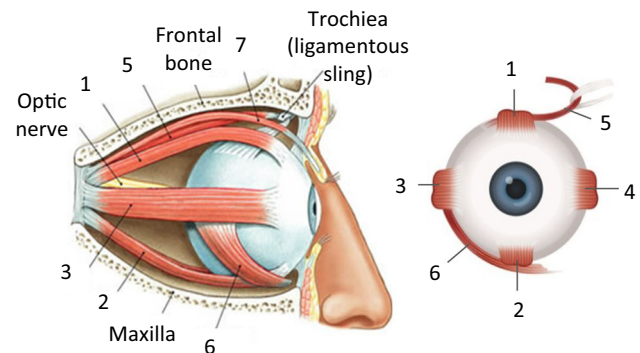

Fig. 4 Eye muscular system [6]. Seven muscles of the orbit: (1) Superior rectus, (2) Inferior rectus, (3) Lateral rectus, (4) Medium rectus, (5) Superior oblique, (6) Inferior oblique, (7) Levator Palpebrae Superioris. *Source*: https://anatomyinfo.com/eye-muscles/ (Accessed: Feb. 8, 2023)

is to retract and release the superior eyelid. It is attached to the sphenoid bone and the tarsal plate in the eyelid. Human eye movements, allowed by the action of the eye muscles, can be classified in three types:

- *Vergence movement*: This is the synchronized movement of both the eyes. Its function is to make sure that the image of the object being looked at falls onto the corresponding spot on both retinas. The motion speed of this movement is around 25 deg/s.
- *Saccadic movements*: These are the most rapid movements of the eyes, used to move quickly from one location in a visual scene to another, during which time visual perception is suppressed. Saccadic speed is about 600 deg/s.
- *Pursuit/Smooth Pursuit movement*: This is activated while tracking an object in motion and speed is comparable to Vergence motions.

Concerning the eye RoM, it changes in each direction and decreases significantly with the age of a person [6]. Usually, to check the health of the eyes, medical tests are carried out in unnatural conditions (for instance, one eye is closed). Thus, they are not a good reference to understand the real
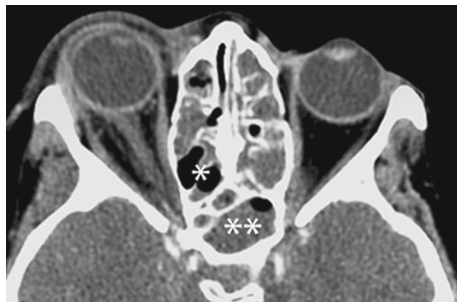
Fig. 5 Example of unilateral proptosis. *Source*: http://www.aao.org (Accessed: Feb. 8, 2023)

eye behaviour [7]. For these reasons average measures were considered in designing EYE-MECH.

Proptosis: This is a bulging of the eye from its normal position in the socket, as shown in Fig. 5. It can be either bilateral or unilateral and the disease seriousness measurement is assessed using an exophthalmometer. Proptosis can be caused by a partial dislocation of the eye from the orbit caused by trauma or a tumorous mass which pushes the eyeball outwards. Trauma affecting the socket can cause a bleeding behind the eye, a dangerous condition called *retrobulbar haemorrhage*. Such non-compressible bleeding may occur rapidly, so pressure grows and pushes the eye forward. The process that causes the eyeball displacement is restricted by the eyelid and can cause compartment syndrome as intra-orbital pressure rises, squeezing the optic nerve and blood vessels, with the potential to cause blindness. According to [8], unilateral proptosis is a critical sign that must be dealt in its early stage. The maximum displacement of the bulging can be estimated at $15mm$. Surgical treatment for proptosis associated with facial trauma is Lateral Canthotomy and Cantholysis (LCC). This procedure is used to decompress compartment syndrome of the orbit by releasing the constraint of the lateral canthal tendon, allowing the globe to move forward more freely until the haemorrhage is resolved. Also, proptosis can be a post-surgical complication in the treatment of an orbital tumour [9]. Bleeding can occur immediately after the surgery, with a peak incidence during the following days. When unresponsive to medicines, the simplest and most effective method to reduce intraocular pressure is the LCC.

2.2 Iris and pupil

The visible dynamic portion of the human eye globe, as shown in Fig. 6, is composed of the iris and the pupil. Their movements, dimensions and structure type are studied in detail below.

Iris: This is a coloured membrane that works as a diaphragm controlling the pupil dimension and the amount of light that reaches the retina. The iris is located within the
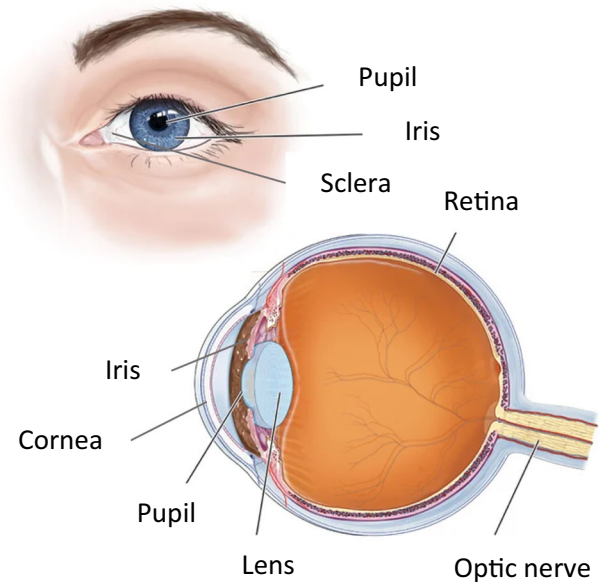

Fig. 6 Human eye: iris and pupil. *Source*: https://my.clevelandclinic.org/health/body/24317-pupil-of-the-eye (Accessed: Feb. 8, 2023)

aqueous humour, between the cornea and the lens. It consists of three main layers: the *endothelium*, the *stroma*, and the *pigmented epithelial cells*.

- The *endothelium* is found on the external face of the iris and is continuous with the endothelium of the cornea.
- The *stroma* is pigmented fibrovascular tissue underneath the epithelium and is the iris' biggest part. It consists of connective tissue and attaches to a sphincter muscle responsible for contracting the pupil, and a dilator muscle formed of radially oriented fibres which pulls the iris in the radial direction to widen the pupil.
- The *pigmented epithelial cells* form the heavily pigmented layer behind the stroma, two cells thick, which prevents the passage of light through the iris to the retina.

The outer edge of the iris is attached to the sclera and the anterior ciliary body [10, 11].

Pupil: This is a variable diameter hole in the centre of the iris which allows light to enter the ocular bulb. Its dimension is regulated, depending on the light intensity, by the iris muscles controlled by the autonomic nervous system. The pupil image seen from outside the eye does not exactly correspond to its actual location and size since it is magnified by the cornea [12]. The dimension variation of the pupil is mainly related to changing light intensity, shifting gaze between closer or farther objects, and sometimes to experiencing emotions such as fear. Closure happens when the sphincter pupillae muscle contracts, pulling the inner iris tissues closer together and constricting the pupil. The dilator
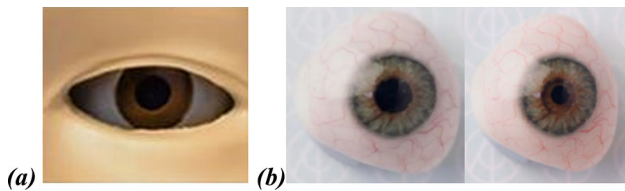
Fig. 7 Example of pupil systems. **a** Manually set; **b** Wide/narrow selectable prosthesis [20]

pupillae, the antagonist of the sphincter pupillae, causes the pupil to dilate. Both muscles are innerved by the sympathetic system. Pupil dimension also varies from person to person and depends on age. An average adult pupil diameter measures from around 2 mm (narrow pupil) to 8 mm (wide pupil), and the external diameter of the iris is around 11.5 mm [13].

3 State of the art

In medical robotic simulation, variation of pupil diameter has been simulated through a Liquid Crystal Display (LCD) monitor in which the pupil and the iris are represented. In this way a lack of realism occurs since the pupil is not a real hole but only a surface part of the LCD monitor [14–19]. Another method to design robot eyes employs a strip with differently sized holes that are mechanically moved into position to simulate different pupil dimensions or conditions [20] (Fig. 7a). Examples of mechanical irises are provided in [21, 22]. In eye prostheses the pupil is normally passive (i.e., not dynamic), however in [23], a pupil with magnetic activation is developed, but the mechanism is manually operated and not progressive, having only two switchable configurations, i.e., narrow, and wide (Fig. 7b). The following paragraphs briefly recall some projects available in the scientific literature concerning the eye motion system design of a robot.

Robot-Cub [24–26] is a component of a humanoid robotic platform, the so-called iCub, aimed at studying human cognition. The robot's size is based on that of a two-year-old child. The eye motion system of the iCub head is shown in detail in Fig. 8a: it comprises 3-DoFs since both eyes can move left/right independently and up/down simultaneously.

KASPAR [27, 28] is a minimally expressive robot suitable for human–robot interaction studies. Its integrated eye motion system is visible in Fig. 8b: it provides the eyes with 3-DoFs, i.e., pitch, yaw, and blinking motion of the eyelids.

MAC-EYE [29, 30] was designed at the University of Genoa to simulate saccadic and smooth pursuit movements. Its motion mechanism is part of a robot bionic vision system, aiming at simulating the human eye movements and solving problems of vision instability during the robot activity. The MAC-EYE structure is shown in Fig. 8c. The eyes are provided with 3-DoFs thanks to four independent tendons driven

by four DC motors. The robot eyeball is bigger than a human one to host a commercial CMOS camera.

The robotic bionic eye designed at Shanghai University shown in Fig. 8 [31] was conceived with a mechanical structure like the human one. The eyeball motion is implemented by a rotational servomechanism. Two additional DoFs for the vertical movement of the structure and the dilatation/contraction of the pupil are provided via RC servos and based on the direction of the light source through a light sensor. Also, a camera is integrated in the eyeball.

Other humanoid robotic eyes have been designed to reproduce the three rotations of the eye driven by pneumatic artificial muscles [32], and to obtain a wide range of motion with high precision simulating the action of vertebrate extraocular muscles [33]. In [34, 35] both the behaviour and appearance of the humanoid robot were investigated to improve the relationship between the robot and the user. The former focuses on the design of bioinspired actuators to achieve horizontal, vertical, and circular motion of the eyes (note that these directions lay on the pupil surface, i.e., they do not include an outside motion perpendicular to the face) while the latter presents a device with 9-DoFs, of which five are for the eye. Gaumard's Hal and related robots use a mechanical pitch/yaw eye motion system; the Pediatric HAL eyes are able of replicating several emotional states, trauma, and other neurological conditions [36]. Also, a bioinspired tendon-driven robot-eye is presented in [37] to improve visual perception; the ocular motion is simulated via the Listing's law principle, reproducing saccades and smooth pursuit action.

The systems described, simulating either an eye apparatus or a pupil, are not suitable for a medical simulator. In fact, even if their DoFs match the capability of a human eye, the overall eye mechanism structure including the actuators, is not designed to fit inside a medical simulator where invasive procedures are performed. Moreover, proptosis simulation is not considered in any case. Thus, a mechanism accurately replicating human features, both their functions and aesthetics, is needed to replace human beings with a training simulator.

In combination with pitch and yaw mechanisms, one of the main features of the design presented here is the simulation of the proptosis motion. In the case of unconscious patients, the globe should be movable in pitch and yaw when manipulated with surgical instruments, whereas for the conscious ones, the globe may display controlled motion. When retrobulbar haemorrhage occurs, the eye is pushed forward and loses its mobility due to the increased pressure. Once relieved, some of the motion returns.
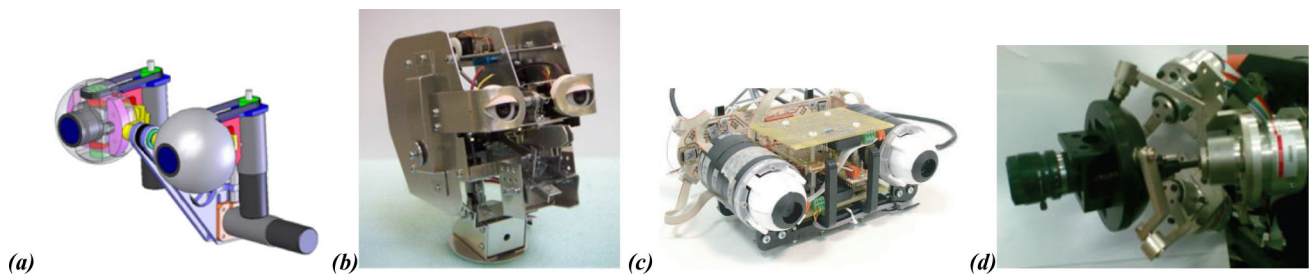
Fig. 8 Example of robotic eye mechanisms. **a** iCub [25]; **b** KASPAR [28]; **c** MAC-EYE [29]; **d** Bionic robotic eye [31]

4 EYE-MECH design and prototype

Basing upon the human eye anatomy studied in detail in Sect. 2, this section focuses on a novel OCF eye system design, aiming at replicating human behaviour, thus, giving the feeling to surgeons/first responders of training on a real patient.

4.1 Proof of concept

Aiming at reproducing a system with the same DoFs as the human eye, the EYE-MECH is designed including all of the motion features of the human eye relevant to eye trauma, namely:

- *Eye pitch and yaw*.
- *Proptosis*.
- *Back driveability in pitch and yaw*, to allow the surgeon to manipulate the eye.

In addition, a force sensing system was realized to detect pressure/load applied to the globe and the force reduction on the eye expected upon successful LCC. The proposed EYE-MECH design aims at solving the challenges of the human eye motion system. The CAD model and the physical prototype of the complete EYE-MECH have been previously introduced and shown in Fig. 3. A single-eye mechanism was initially designed; once a successful result was achieved, the model was duplicated. Under the EYE-MECH project requirements, the mechanism was provided with a RoM of 60° for each of the pitch and yaw rotations, centred at their neutral positions, and with a translational motion of 15 mm for proptosis. The complete assembly of the single EYE-MECH and its exploded view are shown in Fig. 9. The parts were made primarily using 3D printers (Objet 260 V and Dimension Elite, Stratasys, Rehovot, Israel) to ease the complex geometry manufacturing. A *platform (1)* can rotate about all axes on a spherical joint. The platform hosts the front portion of the eyeball and provides the eye with the pitch and yaw motions. It is moved by *tensioned elastic wires (3)* attached at its outer edge and pulled by *actuators (5)* from the back
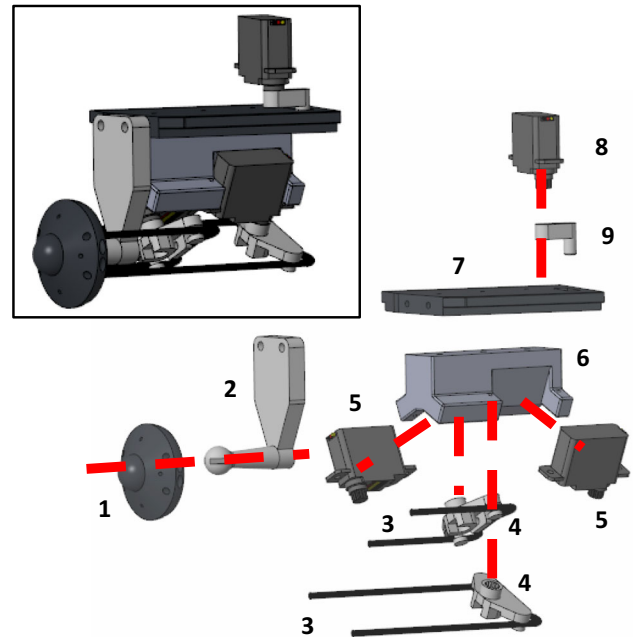

Fig. 9 EYE-MECH assembly and exploded view. (1) Eyeball platform; (2) Triangular support; (3) Neoprene wires; (4) Servo arm; (5) Servo (pitch and yaw); (6) Servo support; (7) Base plate; (8) Servo (proptosis); (9) Proptosis crank

of the mechanism. The elastic linkage aims to simulate the orbital muscles and to allow the passive motion of the eye. This sub-system provides the eye with the rotational motions. In turn, it is moved forward and back on a *flat plate (7)* by an additional actuator and a crank-slider mechanism, forming a second sub-system which generates the proptosis motion.

4.1.1 Pitch and yaw sub-system

In this section the design process for the pitch and yaw mechanism development is analysed.

Actuation System Definition: To provide the eyeball with two independents rotational DoFs, two actuators are needed. The following points report the main issues concerning the actuation system.

Table 1 Servo datasheet (HS-5045HB)

Motor type	3 Pole Ferrite
Bearing	Top Ball Bearing
Gears	Karbonite
Torque@4.8/6.0v	13.88/16.66 oz/in
Speed@4.8/6.0v	0.12/0.10 s for 60 deg
Size	$0.92'' \times 0.38'' \times 0.88''$
Weight	0.29 oz

- *Human anatomy-based*: As already mentioned, the EYE-MECH design aims at being functionally as close as possible to the human eye. Thus, an elastic linkage activated by motors, which pulls the eye platform and makes it pivot on the spherical joint, was implemented. Through this connection, the functions of the orbital muscles are simulated, within the constraints of fitting the whole system within the envelope of a real skull.
- *Reduced size and weight*: As other devices and systems of the OCF were determined to be mounted within the skull (audio speaker, jaw motion mechanism, fluidic distribution system for simulated haemorrhage), a goal of the eye motion design was compactness.
- *Reduced noise and vibrations*: To avoid distracting from the realism of a training scenario, one issue for consideration is minimizing noise and vibration from the actuation system.
- *RoM and speed*: Actuator specifications were chosen to match motion requirements and provide the eye with the proper RoM. It is worth noting that the RoM of the eye is not the same as that of the actuators since the transmission ratio of the elastic linkage need not be 1:1. The actuator's range of speed is designed to be wide enough to allow the simulation of a saccade motion of the eye (Sect. 2.1). Slower motions may be obtained by simply reducing the commanded speed.

Multiple options are available for the pitch-yaw mechanism. In the case of linear motors, considering that the transmission is made of preloaded elastic wires, at least three actuators would be needed to provide motion and maintain uniform tension. Alternatively, choosing rotary actuators with suitable cranks allows use of only two servos. To satisfy project requirements, two miniature RC servos, typically used in aeromodelling, were selected for the pitch and yaw motions. The servos used were two HS-5045HB digital servos (HiTek, RCD USA, Inc., San Diego, CA), and their specifications are reported in Table 1. The ranges of speed (600 deg/s) and torque are a reasonable value for the saccade motion (Sect. 2.1).

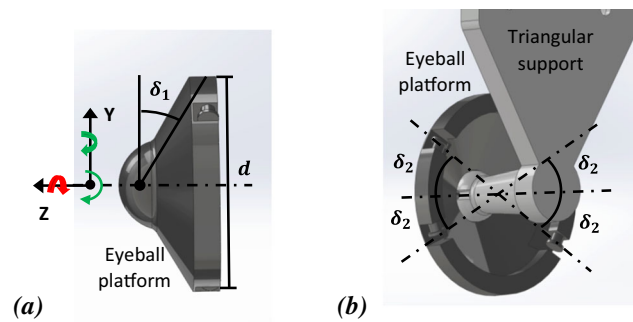**Mechanism Design Concept:** As previously said and shown in Fig. 9, the system is made of a rotating platform,

Fig. 10 a Eyeball platform, $d = 24$ mm. Conical shape ($\delta_1 = 30°$). 2-DoFs in green (pitch and yaw), one fixed rotation in red (rolling). **b** Elbow platform and triangular support assembly (spherical joint). Four attachments for the elastic transmission ($\delta_2 = 25°$)

to which the silicone eyeball attaches, actuated via an elastic transmission.

As visible in Fig. 10a, the *eyeball platform* (Fig. 9, (1)) has a diameter $d = 24$ mm, approximately equal to the mean of transverse and vertical diameters of the average human adult eyeball [38]. The conical shape was realized with an angle $\delta_1 = 30°$ to find a compromise between the desire for a full spherical eye globe, and the need to provide enough space to satisfy the RoM project requirement ($\pm 30°$). The platform has a spherical cavity at its centre and snaps onto the complementary part of the joint (Fig. 10b), as it's opening subtends an angle slightly bigger than 180°, i.e., 200°. Inside this cavity are two tiny cylindrical pins to prevent the rolling/torsional movement of the platform (see Fig. 10a for the rotational DoFs of the eyeball). These pins mate with grooves in the spherical tip of the triangular support, on which the platform rotates.

The *triangular support* is an L-shape part with a conical pin (Fig. 9, (2)). The conical pin has a spherical tip that mates with the platform cavity. To reduce friction between the components during motion, a radial gap of 0.12 mm between the platform and the pin has been set. The conical pin length, thickness, and taper angle (4° of inclination) have been chosen to prevent collision with the platform over the complete RoM and resist bending moments. The triangular support was designed to avoid interference with the elastic wires and to provide a robust connection to the rest of the assembly. The triangular portion of the support acts as a cantilever beam when axial loads are applied to the eyeball, as when proptosis is simulated or when a first responder inappropriately presses on the eyeball. Deflection of the beam caused by applied force is measured using a strain gage bonded to the beam's surface (see Sect. 4.1.3).

The triangular support is attached to a *rectangular flat plate* (Fig. 9, (7)), which rides between linear bearing surfaces (not shown), using two screws. Since the mechanism
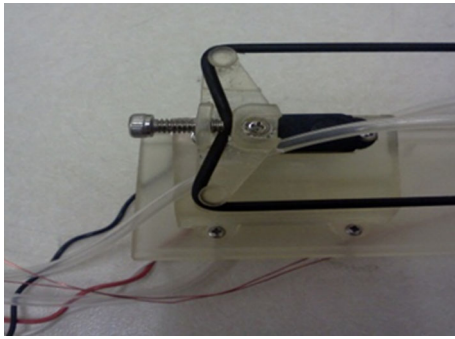
Fig. 11 Arm support physical prototype with neoprene wires

was designed to make efficient use of available space available in the skull, the flat plate was positioned above the eye, occupying the lower portion of the cranial vault. The flat plate hosts the *actuators supports* (Fig. 9, (6)) and longitudinal slots that mate the pitch and yaw sub-system with the proptosis sub-system. Together, the size of the flat plate/L-shaped part/actuator/eyeball platform assembly of the pitch and yaw sub-system is approximately $76 \times 35 \times 47$ mm. The slots along the sides of the flat plate slide into a track in the proptosis mechanism A second slot in the body of the flat plate mates with the crank (Fig. 9, (9)) that drives proptosis motion. This concept will be clarified in the next section with the introduction of the proptosis sub-system (Sect. 4.1.2., Fig. 12). *Two rotational servos* (Fig. 9, (5)) transmit their movements to elbow-shaped *arm supports (4)*, that pull and stretch the *neoprene wires (3)*, thus, driving the eyeball platform in the pitch and yaw directions. The arm supports, which may be seen in detail in Fig. 11 include splines which mate with the servo output shafts. The actuator support holds the actuators firmly and keep them in the correct location. It is designed with an inverted Y-shape to hold the servos in inclined positions and is tightened to the base plate with a couple of screws. The Y-shape of the actuator support aligns the arm supports with the centre of the spherical joint.

In turn the elastic wires, made of neoprene to simulate the elasticity of the orbital muscles, wrap around pins at each end of the arm supports, are terminated in holes in the eyeball platforms, and are retained and tensioned using set screws. To provide the required motion of the eyeball, the pins are set at the same radial distance as the holes in the eyeball platform and at the same 30° inclination.

While independent pitch and yaw motion can be achieved, as the eye does, with orthogonal wire (or muscle) attachments at horizontal and vertical sites on the eyeball, the triangular plate and actuators obstruct this configuration. Instead, after simulating alternatives, the Y-shaped configuration of the actuator support was selected, which aligns the servos and arm supports at $\pm\delta_2 = 25°$ from the horizontal axis (Fig. 10).

Good motion control is achieved by coupling servo motions to achieve pitch, yaw, and combined motions. Rotation of the actuators in the same direction provides the eye with pitch motion, whereas the yaw motion is achieved through actuator rotations in opposite directions. The control law to move the actuators to reach an eye configuration may be obtained via trigonometric considerations as reported in Sect. 4.2. Since the servos are mounted at different distances from the eye platform, the elasticity of the additional length of the neoprene wires results in the need for larger rotation of the more distant actuator to achieve the same eye platform rotation as from the closer actuator; this is included as an additional factor after the pure trigonometric control law is calculated.

Transmission System: The transmission described above allows the rotational motion of the eyeball platform by converting servo torques into a net torque applied to the eyeball. An elastic connection, rather than a rigid one, allows the required capacity to move the eye with surgical instruments, but it is less reliable from both position control accuracy and frequency response points of view, allowing the potential for longer oscillation of the body before reaching the final position [39]. As a design choice, aiming at realizing a visually realistic system can be prioritized overachieving an extremely precise mechanism.

In considerations of the material for the elastic elements, Young's Modulus of the neoprene was not specified by the supplier, so a test to evaluate it was made. Wire elongation under different load conditions was analysed. A neoprene wire of 50.8 mm length with a cross section of 2.7 mm^2 was cut from a coil. One end of the wire was fixed with a clamp, and a small, transverse hole was made in the other. Via this hole, several weights were attached to the wire to measure different elongations and compute the Young's Modulus [41]. The test was done at five different total weights, i.e., 0.1 kg, 0.2 kg, 0.3 kg,0.4 kg, and 0.5 kg. Each test was repeated three times and an average of the elongations was calculated. For each weight, Young's Modulus was calculated, and the five values were averaged resulting in a value of approximately 4.2 MPa. A stress-elongation diagram was generated using Excel (Microsoft Corp., Redmond, WA); it had a linear shape, in accordance with the expected linearly elastic material properties over the range of loads and reported values for neoprene [40].

4.1.2 Proptosis sub-system

The proptosis sub-system design is presented in this section, which moves the eyeball and the pitch and yaw sub-system backward and forward. This translational DoF is independent of the pitch and yaw motions, so the pitch and yaw sub-system can be considered as a passive mechanism carried forward and back with a RoM of about 15 mm. Rather than linear
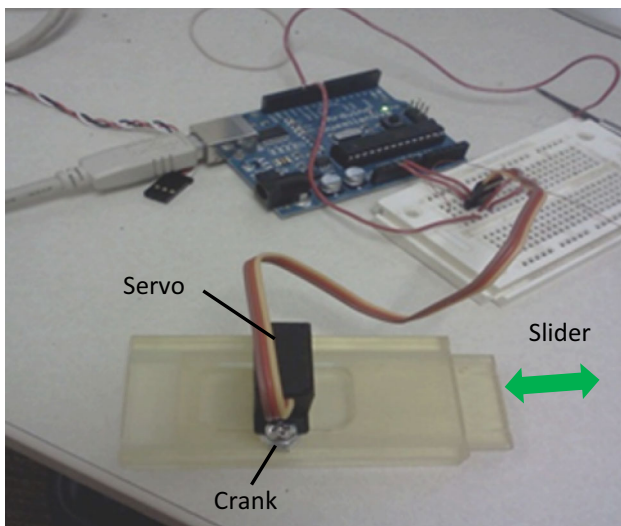
Fig. 12 Proptosis sub-system physical prototype

4.1.3 Load sensor

A load sensing system is integrated into the EYE-MECH to track forces applied to the eye by the trainee's interventions, whether releasing pressure during treatment of retrobulbar haemorrhage or inappropriately applying pressure. Loading along the Z-axis, (Fig. 10) through the spherical pivot causes the cantilevered triangular support to be bent and its deformation detected by a strain gauge (Fig. 13). To estimate the load applied to the eye, the preload of the elastic connections must be deducted from the total load which causes the triangular support to deflect. With a neoprene wire cross section $A_{cross} = 2.7\,mm^2$, and given two wire attachments for each of two wires at the eyeball platform, the total area A_{tot} is
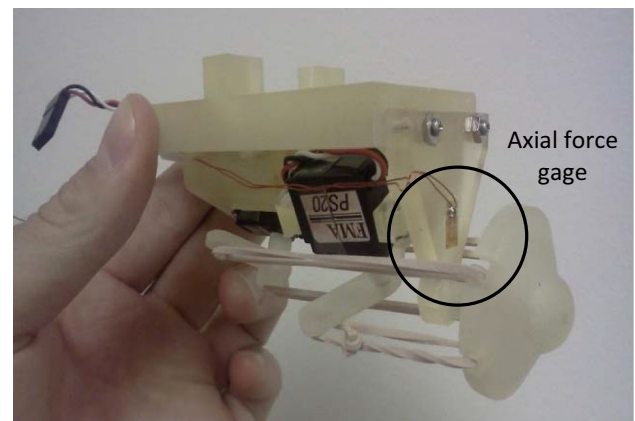
actuation, it was decided to use a servo motor to conserve space. While this requires conversion from rotary motion, it includes several advantages.

Using servos for all three DoFs simplifies the control system; numerous easily programmable microcontroller boards support simultaneous control of multiple RC servos. Also, the low size and weight of the servos selected minimize the overall fixed to the upper part of the skull includes a track, within which the base plate of the pitch and yaw sub-system rides, and the mechanism dimensions. The proptosis sub-system crank-slider mechanism [42] is shown in detail in Fig. 12. A case proptosis *servo* (Fig. 9, (8)). The *crank* (Fig. 9, (9)) is a modified RC servo "horn" which engages a transverse slot on the base plate, forming a Scotch yoke mechanism. The 7.5 mm radius of the crank combined with a 180° servo rotation yield the proptosis sub-system's desired 15 mm RoM. The HS-5045HB servos used in the pitch and yaw sub-system were also suitable to meet the proptosis sub-system requirements, further simplifying assembly.

Fig. 13 EYE-MECH prototype with strain gauge attached in the triangular support

(Eq. 1):

$$A_{tot} = nA_{cross} = 10.8\,mm^2 \tag{1}$$

where $n = 4$ is the number of neoprene wires attachments.

With a 20% stretch preload in the neoprene wires, i.e., $\varepsilon_n = 0.2$, and a Young's Modulus of approximately 4.2 MPa, a stress value $\sigma_n = 0.84$ MPa may be obtained. So, the force due to the transmission wires is computed as follows:

$$F_n = \sigma_n A_{tot} = 9N \tag{2}$$

Assuming the force to be detected F_d was about $1.5N$ or $2N$, the total load applied to the eye which must be tracked by the sensor system is found as in Eq. 3:

$$F_{tot,n} = F_n + F_d \approx 11N \tag{3}$$

The choice of using neoprene wires resulted in a reliable transmission. The strain gauge (see Table 2) was epoxied to a site on the central zone of the triangular support (Fig. 13) which had been sanded and cleaned to ensure adhesion.

4.2 Kinematics

To correctly control the movements of the prototype, a kinematic model was developed, and the corresponding laws of motions needed to program the Arduino were determined. In the following paragraphs, for a generic quantity x, $\cos x = cx$ and $\sin x = sx$.

4.2.1 Pitch and yaw

The eye mechanism can rotate in both the yaw (α) and pitch (β) directions, under the control of the two independent servos, with rotations θ_1 and θ_2. As shown in Fig. 14,

Table 2 Gage datasheet

Description: General-purpose gage. Exposed solder tab area: 1.8×1.0 mm

Gage dimensions (mm)

Gage length: 1.57	Overall length: 5.59	Grid width: 3.05	Overall Width: 3.05	Matrix length: 7.9	Matrix width: 4.8
Gage designation			Resistance (Ohms)		
CAE-XX-062UW-120			$120 \pm 0.3\%$		
CAE-XX-062UW-120			$350 \pm 0.3\%$		
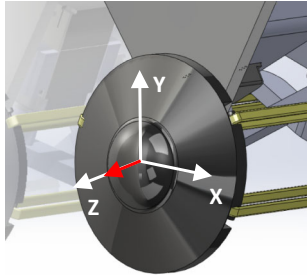
Fig. 14 Polar coordinates system fixed to the eyeball platform (GCS (XYZ), white); unit vector (red) (colour figure online)
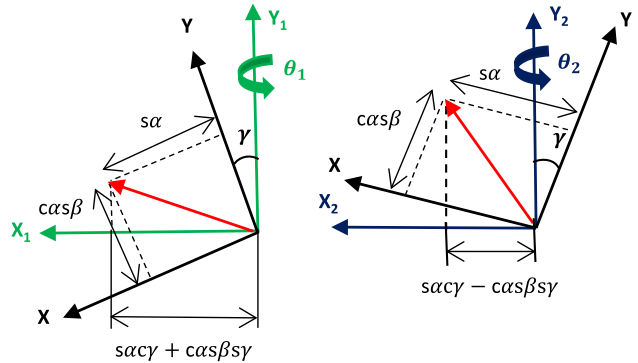
Fig. 16 YX-plane. Vector components in $CS_1(X_1Y_1Z_1)$ and CS_2 ($X_2Y_2Z_2$) (green and blue, mobile) (colour figure online)
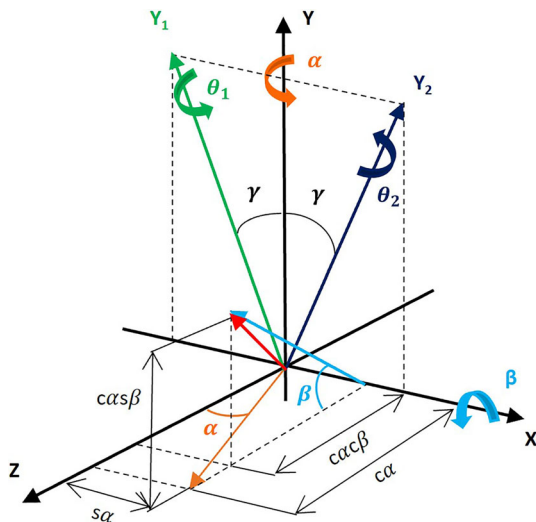
Fig. 15 Generic position of the eyeball (unit vector, red) in $GCS(XYZ)$ (black, fixed) (colour figure online)

Fig. 17 XZ-plane. Vector components in $CS_1(X_1Y_1Z_1)$ and CS_2 ($X_2Y_2Z_2$) (green and blue, mobile) (colour figure online)

the orientation of the eyeball is shown by a unit vector (in red) with reference to a fixed coordinate system $GCS(XYZ)$ (in white), whose origin is the platform's centre of rotation. The unit vector lies on the Z-axis in the initial position. Any other vector position can be determined by projecting the unit vector onto the XZ plane to define α, and onto the YZ plane, defining β (Fig. 15). Referring to Fig. 15, a mobile reference system, $CS_i(X_iY_iZ_i)$, is defined for each servo, whose axis of rotation, Y_1, is oriented at $\gamma = 25°$ away from the fixed Y-axis of GCS (positive for servo 1, negative for servo 2) in the YX-plane. When $\alpha = \beta = 0$, all the Z-axes are

colinear. For any desired orientation of the eyeball platform, both CS_i ($i = 1, 2$) rotate about Y_i such that the (red) unit vector remains on each Y_iZ_i-plane. This is possible thanks to the mechanism design detailed in Sect. 4.1.1.

As shown in Fig. 16, the length and inclination of the arms connected to the servos are the same as those of the attachments of the rotational platform relative to its centre. To find the rotation θ_1, the projections of the unit vector in its final position on the fixed Z-axis and on the X_1-axis are derived. The first projection is shown in Fig. 15 and is equal to $c\alpha c\beta$. The second projection, equal to $s\alpha c\gamma + c\alpha s\beta s\gamma$, may be deduced by geometric considerations shown in Fig. 16. Using the same approach, the X_2-component of the unit vector is computed as $s\alpha c\gamma - c\alpha s\beta s\gamma$. Referring to Fig. 17,
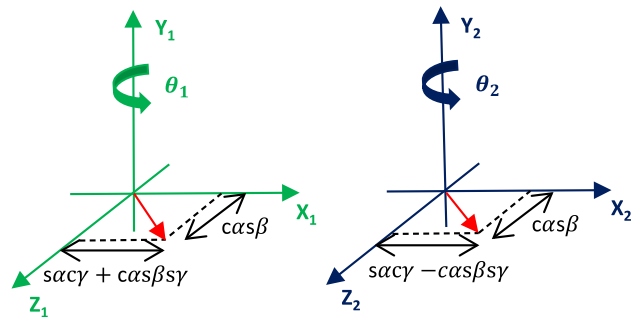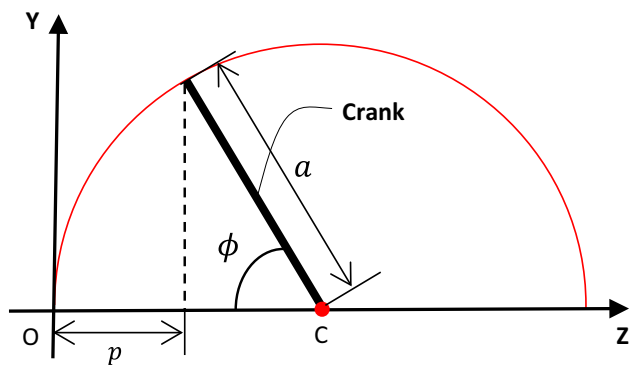
Fig. 18 Proptosis motion scheme (*Z*-*Y* plane)

Eqs. 4 and 5 are computed. Thus, the servo angles θ_1 and θ_2 for any given α, β and γ may be found through the inverse tangents of Eqs. 4 and 5.

$$\tan\theta_1 = \frac{s\alpha c\gamma + c\alpha s\beta s\gamma}{c\alpha c\beta} \tag{4}$$

$$\tan\theta_2 = \frac{s\alpha c\gamma - c\alpha s\beta s\gamma}{c\alpha c\beta} \tag{5}$$

Note as the servos rotations are functions only of α, β and γ (in this case, $\gamma = 25°$).

4.2.2 Proptosis

To control the EYE-MECH proptosis sub-system, the crank angle is related to the sliding position of the system. Referring to Fig. 18, *a* is the length of the crank and ϕ is the angle between the crank and the *Z*-axis about C, the crank centre of rotation. For the eye in its normal position, displacement $p = 0$, and $\phi = 0$. For maximum proptosis, displacement $p = 2a$, from the origin occurs and $\phi = 180°$. The generic crank position *p* may be formulated as in Eq. 6:

$$p = a(1 - c\phi) \tag{6}$$

4.3 Eye pupil

The eye pupil mechanism design was developed with the main features and requirements below:

- *Human anatomy-based*: the mechanism is designed to appear as realistic as possible, both in terms of the external and internal features that surgeons may come across during operations.
- *Small size*: the mechanism should fit inside the eye bulb and be attached to the EYE-MECH. This point is one of the main design constraints.
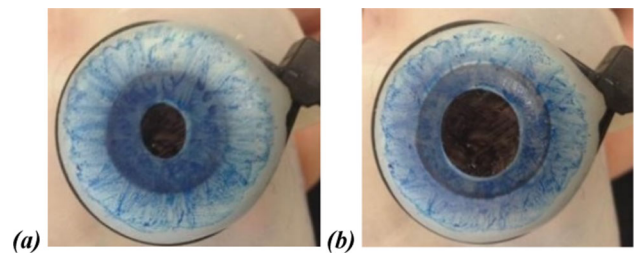

Fig. 19 Eye pupil, membrane system. **a** Narrow, and **b** open-wide configuration
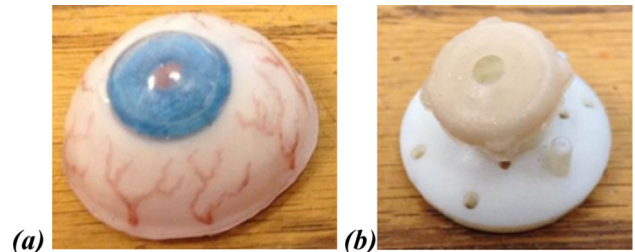

Fig. 20 Prototype of the pupil system. **a** Iris membrane; **b** bulb assembly: ring and cylinder (eye holding structure)

- *Movement simulation*: the opening and closing of the iris should be reproduced to provide the mannequin with an active iris.
- *RoM requirement*: the RoM should be the same as that of the human iris.
- *Light response*: a light sensor should be provided, and the controller should cause the pupil dimension to change according to variation in brightness in the environment.

Solutions found in the literature were not compatible with the pitch and yaw sub-system (e.g., [22]). A solution that fits features such as reliability and ease of manufacturing better was developed and prototyped (Fig. 19). The RoM corresponds with the parameters described in Sect. 2.2 ($d_{min} = 2$ mm for a narrow pupil, $d_{max} = 8$ mm for a dilated pupil). The pupil is formed as a hole in an elastic membrane, emulating a real eye's structure, and fitting within a silicon eye bulb. The prototype of the eye bulb system is shown in Fig. 20. The internal structure was 3D printed, whereas the bulb and the iris were cast in silicon. The version shown has a completely transparent bulb to show the iris, the inner surface of which was painted to resemble a normal iris. An axially aligned cylinder, about which the iris is mounted, can host a light sensor, and may be painted black. The whole system is attached to the EYE-MECH and fits inside the OCF skull (Fig. 3). Figure 19 shows the mechanical deformation of the thin silicon layer and variation in pupil size. This deformation is caused by downward translation of a rigid ring link, which slides on the hollow cylinder. The iris is a thin silicone "cap" with a central hole, which is attached to the ring link.
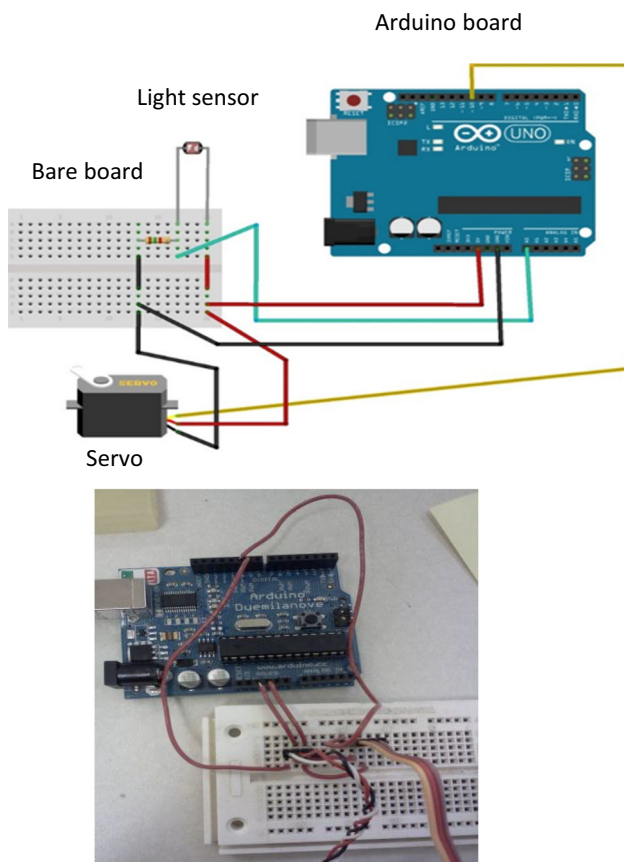
Fig. 21 Arduino controlled pupil deformation scheme

Fig. 22 EYE-MECH motion control GPC (Blue grid: X-axis, yaw (α); Y-axis, pitch (β). Orange grid: proptosis (p)). Physical prototype schematics: system motion versus GPC imposed target positions: A ($\alpha = -30°$, $\beta = 0°$), B ($\alpha = 0°$, $\beta = -30°$), C ($\alpha = \beta = 0°$, $p = 14$ mm)

The downward translation of the ring forces the silicon to stretch and widen the hole, thus dilating the pupil. Silicones of different durometers were tested to achieve an appropriate elasticity in the iris. The ring movement is provided by four wires linked to a servo motor (not shown) that pulls the ring itself, whereas the reverse movement, i.e., the closure, is provided by the elastic recoil of the silicon. The cylinder was realized by modifying the eyeball platform through the addition of five holes (four for the dilation wires and one for the light sensor wiring) and the structural components that extend towards the iris.

4.4 Motion control and tests

Motion control of the EYE-MECH was implemented using an Arduino Duemilanove microcontroller, and a Graphical User Interface (GUI) was realized using Processing [43]. The Arduino is connected to the host computer through a USB cable, which provides for serial communication with the GUI and power.

Figure 21 shows the prototype electronics for the pupil deformation mechanism. A photoresistor placed inside the hollow pupil forms part of a voltage divider, the output of which is sampled by an analogue input pin of the Arduino.
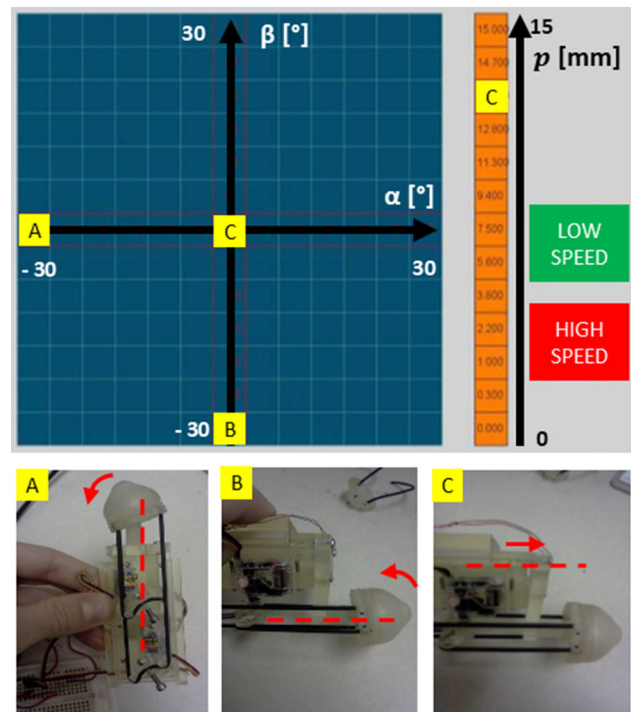
The software uploaded to the Arduino converts the brightness value to a pulse-width modulated output signal sent to the pupil servo which pulls or releases the wires attached to the pupil ring to cause dilation or contraction.

Figure 22 shows the test of the prototype mechanism in different configurations (A, B, C) controlled through the Graphical Panel Control (GPC) GUI. The GPC was designed to provide a simple control interface for EYE-MECH position. The independent eye motions described in Sect. 4.1 may be activated simultaneously or individually through the blue cartesian grid (yaw/α on horizontal axis, pitch/β on vertical axis) and the orange linear scale (proptosis). Pursuit and saccadic pitch and yaw motion speeds are selected by means of the "low speed" and "high speed" buttons on the right side of the control panel (green and red). The software is non-blocking, so new configurations can be selected and motion toward the new target initiated even if the previous movement is not yet finished. During tests in laboratory the system has faithfully acted as designed, since the target positions imposed from the GPC were reached by the physical prototype as measured by offline images analysis. As a next step, the device is to be tested by surgeons for validation and to be used in real applications.

5 Conclusions

This research presents a robotic eye system to be integrated in an OCF simulator for training medics and physicians to give them the feeling of working on a real human body. A dynamic system of the eye has been designed, replicating important human eye behaviours. The eye mechanism includes all the globe motion features, i.e., (1) pitch and yaw, (2) proptosis, (3) back driveability in pitch and yaw, to allow the surgeon to manipulate the eye, and (4) sensing of applied force to detect loads applied to the globe and the reduction of force on the eye expected on successful canthotomy/cantholysis. In further development, additional features will allow replication of a wider range of clinical scenarios. Considering many common craniofacial traumas, interesting areas to focus on may be fractures of the maxilla and mandible, as well as the cervical vertebrae. Considering the invasive procedures on the simulator haemorrhage control and advanced ocular interventions, an important feature to be investigated would be the design of a hydraulic system to simulate bleeding and other human fluid systems, e.g., the lacrimal system and the spinal fluid.

References

1. Montgomery, S.P., Swiecki, C.W., Shriver, C.D.: The evaluation of casualties from operation Iraqi freedom on return to the continental United States from March to June 2003. J. Am. Coll. Surg. **201**(1), 7–12 (2005)
2. Carey, M.E.: Learning from traditional combat mortality and morbidity data used in the evaluation of combat medical care. Milit. Med. **152**, 1–6 (1987)
3. Ottensmeyer, M.P., De Novi, G., Loan, G.: Development of an ocular and craniofacial trauma treatment training system. Technical Report, Massachusetts General Hospital, Boston, USA (2015). https://apps.dtic.mil/sti/citations/AD1007737
4. De Novi, G., Bardsley, R., Shah, R., Ottensmeyer, M.P., Moore, J.C., Ahn, B.: Event-driven surgical gesture segmentation and task recognition for ocular trauma simulation. In: Proceedings of 8th International Conference on Intelligent Environments, pp. 341–352 (2012)
5. Snell, R.S., Lemp, M.A.: Clinical Anatomy of the Eye, 2nd edn. Wiley-Blackwell, New York (2013)
6. Dutton, J.J.: Atlas of Clinical and Surgical Orbital Anatomy. Elsevier, New York (2011)
7. Lim, H.W., Song, Y., Kim, J.H., Shin, Y.U., Hwang, S.J., Hong, S.: Normal range of eye movement and its relationship to age. Investig. Ophthalmol. Vis. Sci. **58**, 747 (2017)
8. Khan, N.H., Moin, M., Khan, M.A., Hameed, A.: Unilateral Proptosis: A Local Experience. Department of ENT and Ophtalmology. King Edward Medical College/ Mayo Hospital, Lahore (2004)
9. Matei, C., Stanila, A.: The surgical treatment of orbital tumors. AMT **2**(1), 169–170 (2012)
10. "Eye, Human", Encyclopædia Britannica (2006)
11. Gold, D.H., Lewis, R.: Clinical Eye Atlas. Oxford University Press, Oxford (2010)
12. Cassin, B., Solomon, S.: Dictionary of Eye Terminology. Triad Publishing Company, Gainsville (1990)
13. Malmström, T., Kröger, R.H.: Pupil shapes and lens optics in the eyes of terrestrial vertebrates. J. Exp. Biol. **209**(1), 18–25 (2006)
14. Chihara, T., Wang, C., Niibori, A., Oishio, T., Matsuoka, Y., Sessa, S., Ishii, H., Nakae, Y., Matsuoka, N., Takayama, T., Takanishi, A.: Development of a head robot with facial expression for training on neurological disorders. In: Proceeding of the IEEE International Conference on Robotics and Biomimetics, pp. 1384–1389 (2013)
15. Prendergast, W.K., Reed, J.T.: Patent Simulator Eye Dilation Device. Patent US5900923A, United States (1999)
16. Courtoy, C., Cote, Y., Charbonneau, E.: Patient Simulating Mannequin Eye Module. Patent WO2012/075166A1 (2011)
17. Group Project: Computer Controlled Eyes for Patient Simulator, Vanderbilt School of Engineering, 2007/2008, http://research.vuse.vanderbilt.edu/srdesign/2007/group8/index.htm. Accessed 10 Feb 2023
18. Genaral Doctror – Emergency Care Patient Simulator, Shanghai Honglian Medical Instrument, China. https://www.medicalexpo.com/prod/shanghai-honglian-medical-instrument/product-77220-745658.html. Accessed 10 Feb 2023
19. Adafruit – Animal Snake Eyes Bonnet for Raspberry Pi. https://learn.adafruit.com/animated-snake-eyes-bonnet-for-raspberry-pi/hardware-assembly. Accessed 10 Feb 2023
20. Eye Examination Simulator, https://www.kyotokagaku.com/en/products_introduction/m82/. Accessed 10 Nov 2022
21. Pupils assessment in SimMan3G. https://www.youtube.com/watch?v=1Il9254ITnw. Accessed 10 Feb 2023
22. Baldrighi, E., Thayer, N., Stevens, M., Echols, S.R., Priya, S.: Design and implementation of the bio-inspired facial expressions for medical mannequin. Int. J. Soc. Robot. **6**, 555–574 (2014)
23. ART LENS, Eye Prosthesis: https://www.artlens.es/lang/EN/new-ocular-prosthetic.php. Accessed 10 Nov 2022
24. iCub: https://icub.iit.it/. Accessed 10 Nov 2022
25. Beira, R., Lopes, M., Praca, M., Santos-Victor, J., Bernardino, A., Metta, G., Becchi, F., Saltaren, R.: Design of the robot-cub (iCub) head. In: Proceeding of the IEEE International Conference on Robotics and Automation, pp. 94–100 (2006)
26. Nestor, E. Nava., R., Metta., G., Sandini, G., Tikhanoff, V., Kinematic and Dynamic Simulations for the Design of iCub Upper-Body Structure. In: Proceedings of the Biennial ASME Conference on Engineering System Design and Analysis, ESDA2008–59082, pp. 413–421 (2008). https://doi.org/10.1115/ESDA2008-59082.
27. KASPAR: The Social Robot. https://www.herts.ac.uk/kaspar/the-social-robot. Accessed 10 Nov 2022
28. Dautenhahn, K., Nehaniv, C.L., Walters, M.L., Robins, B., Kose-Bagci, H., Mirza, N.A., Blow, M.: KASPAR—A minimally expressive humanoid robot for human-robot interaction research.

Appl. Bionics Biomech. **6**(3–4), 369–397 (2006). https://doi.org/10.1080/11762320903123567

29. Biamino, D., Cannata, G., Maggiali, M., Piazza, A.: MAC-EYE: a Tendon Driven Fully Embedded Robot Eye. In: Proceeding of the IEEE-RAS International Conference on Humanoid Robots, 1573546, pp. 62–67 (2005)

30. Cannata, G., D'Andrea, M., Maggiali, M.: Design of a humanoid robot eye: models and experiments. In: IEEE-RAS International Conference on Humanoid Robots, pp. 151–156 (2006). https://doi.org/10.1109/ICHR.2006.321377

31. Zhou, Y., Luo, J., Hu, J., Li, H., Xie, S.: Bionic eye system based on fuzzy adaptive PID control. In: International Conference on Robotics and Biomimetics (2012)

32. Wang, X., Zhang, Y., Fu, X., Xiang, G.: Design and kinematic analysis of a novel humanoid robot eye using pneumatic artificial muscles. J. Bionic Eng. **5**, 264–270 (2008)

33. Cheng, Y., Wang, S., Yu, D.: Optimal design of a parallel bionic eye mechanism. J. Mech. Sci. Technol. **33**(2), 879–887 (2019)

34. Minato, T., Shimada1, M., Ishiguro, H., Itakura, S.: Development of an android robot for studying human-robot interaction. In: International Conference on Industrial, Engineering and Other Applications of Applied Intelligent Systems, IEA/AIE: Innovations in Applied Artificial Intelligence, pp. 424–434 (2004). https://doi.org/10.1007/978-3-540-24677-0_44.

35. Li, L., Godaba, H., Ren, H., Zhu, J.: Bioinspired soft actuators for eyeball motions in humanoid robots. IEEE/ASME Trans. Mechatron. **24**(1), 100–108 (2019)

36. Gaumard – Simulators for Health Care Education, https://www.youtube.com/watch?v=iItOtCrk6GU. Accessed 10 Feb 2023

37. Cannata, G., Maggiali, M.: Models for the design of bioinspired robot eyes. IEEE Trans. Robot. **24**(1), 27–44 (2008)

38. Bekerman, I., Gottlieb, P., Vaiman, M.: Variations in eyeball diameters of the healthy adults. J. Ophthalmol. **2014**, 503645 (2014)

39. Szybka, T., Zagrodny, B., Awrejcewicz, J.: Mechatronic eye: modeling and design. Pomiary Automatyka Robotyka **1** (2013)

40. Mechanical Properties, https://moldeddimensions.com/mechanical-properties.php. Accessed 8 Feb 2023

41. Shigley, J., Mischke, C., Budynas, R.: Mechanical Engineering Design. McGraw-Hill Education, New York (2003)

42. Legnani, G., Tiboni, M., Adamini, R., Tosi, D.: Meccanica degli Azionamenti, Vol.1-Azionamenti Elettrici. Esculapio-Bologna (2008)

43. Welcome to Processing!, https://processing.org. Accessed 10 Feb 2023